CANCER GENOMICS & PROTEOMICS *20*: 567-581 (2023)
doi:10.21873/cgp.20406

# Hsa_circ_0079557 Promotes the Proliferation of Colorectal Cancer Cells Through the hsa_circ_0079557/miR-502-5p/CCND1 Axis

CHAO YU[1#], XUE HUANG[1#], RENLI HUANG[1], PEIQI WANG[1], ZONGDA CAI[2], ZEYI GUO[3], QINGNAN LAN[1], HAODI CAO[4] and JINLONG YU[1]

[1]*Department of General Surgery, Zhujiang Hospital, Southern Medical University, Guangzhou, P.R. China;*
[2]*Department of Gastrointestinal Sugery, First Quanzhou Hospital, Fujian Medical University, Quanzhou, P.R. China;*
[3]*Department of Hepatobiliary Surgery, Zhujiang Hospital, Southern Medical University, Guangzhou, P.R. China;*
[4]*Department of Endocrinology, Zhujiang Hospital, Southern Medical University, Guangdong, P.R. China*

**Abstract.** *Background/Aim: Recent studies have demonstrated the crucial regulatory roles of circular RNAs (circRNAs) in cancer initiation and progression. The sponge mechanism of circRNAs has been shown to be widely active in various types of tumors. However, many circRNAs still have not been verified to function through this mechanism. This study aimed to investigate the regulatory mechanism of hsa_circ_0079557 in colorectal cancer (CRC) and its role in CRC progression. Materials and Methods: Raw gene expression profile datasets were downloaded from Gene Expression Omnibus (GEO) and combined to form a new dataset. Hsa_circ_0079557 was found to be highly expressed in CRC. Its role was evaluated in vitro and in vivo through a series of experiments, including quantitative real-time polymerase chain reaction (qRT-PCR), flow cytometry, colony formation, cell counting kit-8 (CCK-8), transwell assays, scratch wound healing assays, nude mice experiments, and immunohistochemistry (IHC). The association between hsa_circ_0079557 and the identified target microRNAs (miRNA) was confirmed through fluorescence in situ hybridization (FISH) and dual-luciferase reporter assays. The downstream target proteins were predicted using the web-based tool "TargetScan," and their expressions were determined using Western blot (WB). Results: Hsa_circ_0079557 was found to be relatively up-regulated in CRC tissues and cell lines. Suppression of hsa_circ_0079557 expression inhibited cell proliferation in vitro and in vivo. Additionally, hsa_circ_0079557 acted as a "molecular sponge" for miR-502-5p, up-regulating the expression of Cyclin D1 (CCND1). Conclusion: In this study, we identify a highly expressed circRNA in CRC and propose a novel pathway of hsa_circ_0079557/miR-502-5p/CCND1 in CRC.*

[#]These Authors contributed equally to this study.

*Correspondence to:* Jinlong Yu, Zhujiang Hospital, Southern Medical University, Department of General Surgery, No. 253, Industrial Avenue, Haizhu District, Guangzhou City, Guangdong Province, Guangzhou, 510282, P.R. China. Tel: +86 13189097861, e-mail: yujinlong640506@163.com

*Key Words:* Colorectal cancer, CRC, hsa_circ_0079557, miR-502-5p, CCND1, dataset.



Colorectal cancer (CRC) is the third most common malignancy and the second leading cause of cancer-related deaths worldwide (1). By 2030, the global burden of CRC is projected to increase by 60%, with over 2.2 million new cases and 1.1 million deaths (2). Despite significant advancements in radiotherapy, chemotherapy and immunotherapy, the prognosis of patients with CRC remains poor due to late-stage diagnosis, distant metastasis, and chemotherapy resistance (3-6). Therefore, exploring the underlying mechanisms of CRC and developing better therapeutic interventions is crucial.

Non-coding RNA refers to transcriptome RNA molecules that are not translated into proteins (7). Recently, circular RNA (circRNA), a specific type of non-coding RNA, has received significant attention (8). CircRNA has been shown to play diverse roles in breast cancer, esophageal cancer, and gliomagenesis (9-11).

Due to its high stability and conservative nature, circRNA has great potential to serve as a cancer marker (12). Several studies have identified circRNAs as potential targets in CRC (13-15). Moreover, many studies have confirmed that circRNAs can act as sponges for miRNAs, and this mechanism exists

widely (16). For example, circRNA_0000392 functions as an oncogene in colon cancer by sponging miR-193a-5p (17), and circCAMSAP1 acts as a sponge for miR-328-5p in CRC (18).

Bioinformatics analyses are widely applied in RNA biology (19). In this study, we performed a bioinformatics analysis to identify highly expressed circRNAs in CRC. We validated the relatively high expression of candidate circRNAs in cancer tissues and specifically identified hsa_circ_0079557 as a significantly up-regulated circRNA in CRC. Subsequently, we investigated the functional role of hsa_circ_0079557 in promoting CRC cell proliferation and migration. Furthermore, we conducted prediction and validation experiments to identify its target miRNA and downstream protein. Finally, we proposed that hsa_circ_0079557 promotes CRC cell progression by regulating the miR-502-5p/Cyclin D1 (CCND1) axis.

## Materials and Methods

*Patients and specimens*. From October to December 2022, we obtained twenty-three pairs of CRC samples and adjacent normal tissues from CRC patients undergoing surgical procedures at the Department of General Surgery, Zhujiang Hospital, Southern Medical University of Guangzhou, PR China. The experimental protocol was approved by the Ethics Committee of Zhujiang Hospital of Southern Medical University (Ethics number: 2022-KY-189-02).

*Nude mouse xenograft model*. We purchased 4-week-old male BALB/c nude mice from the Guangdong Medical Laboratory Animal Center and raised them under pathogen-free conditions. The nude mice were divided into negative control (NC)-hsa_circ_0079557 and sh-hsa_circ_0079557 groups (n=5 for each group). Sw480 cells ($2\times10^6$ cells per nude mouse) transfected with NC or sh-has_circ_0079557 were subcutaneously injected into the right side of each mouse. After monitoring for two weeks, mice were sacrificed, and tumor sizes were separately calculated in each group using the formula: Tumor size=½ (length × width$^2$). We euthanized nude mice using $CO_2$. The humanitarian endpoint for nude mice was a tumor diameter <2.0 cm. This experimental protocol was approved by the Ethics Committee of Zhujiang Hospital of Southern Medical University (Ethics number: LAEC-2022-025).

*Cell lines*. Human CRC cell lines SW480, SW620, and KM12 and the human normal colorectal epithelial cell line NCM460 were provided by Zhujiang Hospital Laboratory, Southern Medical University. All cell lines were cultured in DMEM (Thermo Fisher Scientific, Waltham, MA, USA) supplemented with 10% fetal bovine serum (Thermo Fisher Scientific), 100 μg/ml penicillin, and 100 μg/ml streptomycin (Thermo Fisher Scientific) at 37˚C in a 5% $CO_2$ atmosphere.

*Bioinformatic analysis*. The raw gene expression profile datasets GSE126094, GSE138589, GSE142837, GSE205643, and GSE121895 were downloaded from Gene Expression Omnibus (GEO: https://www.ncbi.nlm.nih.gov/geo/). We combined these datasets into a new one after eliminating the differences between groups to increase the sample size. We merged the datasets using the R package insilicomerging (DOD: 10.1186/1471-2105-13-335) and removed batch effects using the methodology of Johnson *et al*. (20) to obtain the matrix. This new dataset contained expression information of 2992 Homo sapiens circRNAs in 26 pairs of CRC and adjacent normal tissues.

We used the bioinformatics analysis websites "Circinteractome" (https://circinteractome.irp.nia.nih.gov/) and "Circbank" ( http://www.circbank.cn/ ) to predict circRNA/miRNA interactions and the TargetScan (https://www.targetscan.org) web-based tool to predict downstream target proteins. The possible functional network of differentially expressed circRNAs and predicted miRNAs were constructed using Cytoscape software 3.9.1 (https://cytoscape.org/).

The Kyoto Encyclopedia of Genes and Genomes (KEGG) rest API (https://www.kegg.jp/kegg/rest/keggapi.html) was used to obtain the latest gene annotation of KEGG pathways for gene functional enrichment analysis. We mapped genes to the background set for enrichment analysis using the R package clusterprofiler (version 3.14.3) to obtain the gene set enrichment results.

We used the standardized pan-cancer dataset, The Cancer Genome Atlas (TCGA) Pan-Cancer (PANCAN, N=10535, G=60499), from the University of California Santa Cruz (UCSC) (https://xenabrowser.net/). We extracted the expression data of the ENSG000000110092 (CCND1) gene in each sample and obtained the expression data of 13 cancers with significant differential expression of CCND1.

*RNA extraction, reverse transcription, quantitative real-time polymerase chain reaction (qRT-PCR), and RNase R treatment*. Total RNA was extracted from tissues and cells using TRIZOL reagent (Cwbio, Jiangsu province, PR China). For mRNAs and circRNAs, 1000 ng of total RNA was reverse-transcribed into cDNA using the Evo M-MLV RT Kit with gDNA Clean For qPCR II kit (Accurate Biology, Changsha, PR China). For miRNAs, 1000 ng of total RNA was reverse-transcribed into cDNA using the BIOG miRNA stem-loop RT Kit (BIODAI, Changzhou, PR China). qRT-PCR was performed using a Bio-Rad CFX96TM real-time PCR system (Bio-Rad, Hercules, CA, USA). Primers for circRNAs were designed using the web tool Primer-BLAST ( https://www.ncbi.nlm.nih.gov/tools/primer-blast/index.cgi?LINK_LOC=BlastHome ), Oligo 7 software (https://www.oligo.net/), and CircPrimer software (https://www.bio-inf.cn/). The specificity of primers was tested by Sanger sequencing. Primers for circRNAs were synthesized by Sangon (Shanghai, PR China), and primers for U6 and mRNAs were synthesized by Tsingke (Shanghai, PR China). The relative RNA expression levels were analyzed using the $2^{-\Delta\Delta Cq}$ method (21), with GAPDH as the internal reference gene for mRNA and circRNA and U6 for miRNA. For RNase R treatment, 2 μg total RNA was digested with 3 U/μg RNase R (Geneseed, Guangzhou, PR China) at 37˚C for 20 min and 70˚C for 5 min. Expression levels of linear mRNA and circRNA were determined using qRT-PCR. The primer sequences are listed in Table I.

*Fluorescence in situ hybridization (FISH)*. The hybridization assay was performed using Cy3-labeled hsa_circ_0079557 probes and FITC-labeled hsa-miR-502-5p probes. CRC cells were cultured to 60-70% confluence in laser confocal Petri dishes. Further, cells were washed with phosphate-buffered saline (PBS), fixed with 4% paraformaldehyde, and treated with 0.1% Triton X-100. FISH probes were diluted, denatured, and incubated with CRC cells overnight at 37˚C. The cells were then stained with DAPI-Antifade for 10 min, and the fluorescence signals of the probes were detected using the fluorescence *in situ* hybridization Kit (Ribo, Suzhou, PR

Table I. *Primer sequences for qRT–PCR*.

| Genes | Sequences | |
|---|---|---|
| *GAPDH* | Forward primer | 5'-ACAACTTTGGTATCGTGGAAGG-3' |
| | Reverse primer | 5'-GCCATCACGCCACAGTTTC-3' |
| *hsa_circ_0079557* | Forward primer | 5'-TGAAAGCAAGGAAGTCTGACTCTA-3' |
| | Reverse primer | 5'-AGGTCAGCTGCTTGAACGAT-3' |
| *RAPGEF5* | Forward primer | 5'-TCTTGTGCGTCTAACATCTGC-3' |
| | Reverse primer | 5'-GAATCTGGAACACTTTCGGCTT-3' |
| *U6* | Forward primer | 5'-CTCGCTTCGGCAGCACA-3' |
| | Reverse primer | 5'-AACGCTTCACGAATTTGCGT-3' |
| *miR-502-5p* | Forward primer | 5'-ACACTCCAGCTGGGATCCTTGCTATCTGG-3' |
| | RT primer | 5'-CTCAACTGGTGTCGTGGAGTCGGCAATTCAGTTGAGTAGCACCC-3' |
| | Reverse primer | 5'-CTCAACTGGTGTCGTGGA-3' |
| *miR-330-3p* | Forward primer | 5'-ACACTCCAGCTGGGGCAAAGCACACGGCCTG-3' |
| | RT primer | 5'-CTCAACTGGTGTCGTGGAGTCGGCAATTCAGTTGAGTCTCTGCA-3' |
| | Reverse primer | 5'-CTCAACTGGTGTCGTGGA-3' |

China) according to the manufacturer's protocol. Stained and labeled cells were observed under a fluorescence microscope (Zeiss, Germany). The sequences of the probes are listed in Table II.

*Construction of siRNAs, shRNAs, miRNA mimics, and inhibitors*. Si-hsa_circ_0079557 was obtained from Gene Pharma (Suzhou, PR China), sh-hsa_circ_0079557 was obtained from Hanyi Biotechnology (Guangzhou, PR China), and miR-502-5p mimics and inhibitors were obtained from TranSheepBio (Shanghai, PR China). The siRNAs against hsa_circ_0079557 had the following sequences: siRNA-1: 5'-GCAAGGAAGUCUGACUCUATT-3'; siRNA-2: 5'-GGAAGUCU GACUCUAUCAATT-3'. The sequence of the hsa-miR-502-5p mimics was 5'-AUCCUUGCUAUCUGGGUGCUA-GCACCCAGA UAGCAAGGAUUU-3', while that of the hsa-miR-502-5p inhibitor was 5'-UAGCACCCAGAUAGCAAGGAU-3'. The sequence of the hsa_circ_0079557-NC was 5'-UUCUCCGAACGUGUCACGUTT-3'. The sequence of the mimics-N.C was 5'-UUGUACUACA CAAAAGUACUG-GUACUUUUGUGUAGUACAAUU-3'. The sequence of inhibitor-N.C was 5'-CAGUACUUUUGUGUAG UACAA-3'.

*SiRNA transfection*. For siRNA transfection, $15\times10^5$ SW480 or SW620 cells were seeded in each well of a 6-well plate. After one day, when cell confluence reached 50-70%, cells were transfected with 16.7 nM siRNAs (si-hsa_circ_0079557) or 16.7 nM negative control (NC-si_hsa_circ_0079557) for 48 h using siRNA-MateTM (GenePharma).

*Cell proliferation assay and colony formation assay*. For the cell proliferation assay, transfected SW480 and SW620 cells were seeded into 96-well plates (2,000 cells/well) for 24, 48, and 72 h. At each time point, 10 µl of Cell Counting Kit-8 (CCK-8) solution (DOJINDO, Kumamoto, Japan) was added to each well, and the cells were incubated for 1 h. A multifunctional microplate reader was used to detect the optical density value at 450 nm (BioTek SYNERGY H1, Palo Alto, CA, USA). For the colony formation assay, transfected cells were seeded into 6-well plates (500 cells/well) and cultured at 37˚C for 14 days. Post culture, colonies were fixed using paraformaldehyde for 30 min, then stained with 0.1% crystal violet for 30 min. Cell colonies were counted using the ImageJ software (https://imagej.nih.gov/) and analyzed.

Table II. *Probe sequences for FISH*.

| Probes | Sequences |
|---|---|
| hsa_circ_0079557 | 5' CY3-TGATAGAGTCAGACTTCCTTGC 3' |
| miR-502-5p | 5' FITC-TAGCACCCAGATAGCAAGGAT 3' |

*Migration assay and scratch wound healing assay*. For the cell migration experiment, $10\times10^5$ SW480 and SW620 transfected cells were seeded into the upper chambers of BD Falcon Transwell plates (8-µm pore membranes; BD Pharmingen, Sussex, UK) containing serum-free medium (200 µl), while complete medium (500 µl) was added to the bottom chambers. After one day of culture, the cells in the bottom chambers were fixed with 4% paraformaldehyde and stained with 0.5% crystal violet. The stained cells were then counted under a microscope (Leica DM2500, Weztlar, Germany). Transfected cells were cultured at 37˚C in 24-well plates for the scratch wound healing assay. Scratch experiments were performed using the fine tip of a 10 µl pipette tip. Cells were cultured in DMEM with 1% FBS. Images of migrated cells were captured under a microscope (Leica DM2500) at different time points.

*Luciferase reporter assay*. Both wild-type (WT) and mutant (Mut) hsa_circ_0079557 luciferase reporter plasmids were obtained from TranSheepBio (Shanghai, PR China). The mutant luciferase reporter plasmid (pmirGLO-hsa_circ_0079557-Mut) was constructed by replacing the miR-502-5p binding sequence of the wild-type luciferase reporter plasmid (pmirGLO-hsa_circ_0079557-WT) from "AGCAAGGA" to "AAGGAACT". The mutated sequence was inserted into the pmirGLO plasmid. HEK 293T cells were seeded into 24-well plates ($3\times10^4$ cells/well) in a complete medium and incubated at 37˚C. Negative control or miR-502-5p mimics were then co-transfected into cells with the reporter plasmid using

Lipofectamine 3000 (Thermofisher). After 48 h, cells were lysed with lysis buffer, and luciferase activity was measured using the Dual Luciferase Assay Kit (GeneCopoeia, Rockville, MD, USA). Firefly luciferase was normalized to Renilla luciferase activity. WT or Mut luciferase reporter and miR-502-5p mimics or NC-miR-502-5p were co-transfected into HEK 293T cells.

*Western blotting*. Total proteins were extracted from CRC cells using RIPA lysis buffer (Beyotime, Shanghai, PR China) containing proteinase inhibitors. Proteins were separated using SDS-PAGE (Epizyme, Shanghai, PR China) and then transferred to PVDF membranes (EMD Millipore, Boston, MA, USA). The membranes were blocked with 5% skim milk and incubated overnight at 4˚C with primary antibodies anti-CCND1 (1:1000, Wanleibio, Shenyang, PR China) and anti-β-actin (1:4000, Wanleibio). After washing with Tris-buffered saline for 20 min, the membranes were incubated with horseradish peroxidase-conjugated secondary antibody for 1 h at room temperature. Immunoreactive bands were visualized using a chemiluminescence kit (Wanleibio). β-actin was used as a loading control.

*Flow cytometry assays*. CRC cells were cultured in 6-well plates and transfected with si-1-hsa_circ_0079557 or si-2-hsa_circ_0079557 at 37˚C for two days, then cultured in a serum-free medium for one day. The transfected CRC cells were stained using PI/RNase Staining Buffer Solution (Elabscience, Wuhan, PR China) and detected by CytoFLEX (Beckman, Brea, CA, USA). Cell cycle data were analyzed using FlowJo_v10.6.2 software (https://docs.flowjo.com). Through the software, we can obtain the proportion of G1 phase cells, and then compare the proportion of G1 cells to detect whether there are differences between groups.

*Immunohistochemistry (IHC)*. The PV-6000 kit (ZSGB-BIO, Beijing, PR China) was used for IHC following the manufacturer's protocol. Paraffin-embedded sections were incubated overnight at 4˚C with primary antibodies against CCND1 (1:100, Abcam, Cambridge, UK). After washing with PBS, sections were incubated with anti-rabbit horseradish peroxidase-conjugated secondary antibodies for 1 h at room temperature. Then, they were stained with DAB and hematoxylin and observed with a 3D bright field scanner (HISTECH, Budapest, Hungary).

*Statistical analysis*. Comparisons between groups were analyzed with GraphPad Prism software v9.0 (GraphPad Software, San Diego, CA, USA) with unpaired *t*-tests and one-way ANOVA followed by the Bonferroni post-hoc test. A $p$-Value less than 0.05 was considered statistically significant.

## Results

*Hsa_circ_0079557 is up-regulated in CRC tissues and CRC cell lines*. GSE126094, GSE138589, GSE142837, GSE205643 and GSE121895 were downloaded from the GEO database. We combined them into a new dataset (Figure 1a and b). The merged dataset was then categorized into the tumor and normal group. The differentially expressed circRNAs between groups are listed in Table III, and volcano and heat maps are presented in Figure 1c and d, respectively. Highly expressed circRNAs were selected for further research, and qRT-PCR was conducted. We excluded circRNAs that have been previously studied and found that hsa_circ_0079557 showed the most significant up-regulation in CRC tissues and CRC cell lines (Figure 2a and b). The expression levels of hsa_circ_0079557 are higher in SW480 and SW620 compared to KM12 cells. Hence, we selected hsa_circ_0079557 as the target for further experiments and selected SW480 and SW620 as experimental cells.

Hsa_circ_0079557 contains 565 nucleotides and is derived from exons 2, 3, 4, 5, 6, and 7 of human RAPGEF5 on chr7 (22306582-22357656) (Figure 2c). To validate the qRT-PCR results for has_circ_0079557, we performed Sanger sequencing and confirmed that the head-to-tail PCR splicing product had the expected splicing location (Figure 2d). Furthermore, to establish the stability of hsa_circ_0079557, we performed RNase R treatment, which demonstrated that the level of RAPGEF5 decreased sharply under RNase R treatment compared to hsa_circ_0079557 (Figure 2e). To further confirm the circular nature of hsa_circ_0079557, we performed reverse transcription using Oligo (dT) primers and random primers. The products were tested using qRT-PCR, and the results showed that the level of hsa_circ_0079557 was reduced by Oligo (dT) primers but not affected by random primers (Figure 2f).

*Hsa_circ_0079557 affects the proliferation, migration, colony-forming ability and cell cycle of CRC cells*. To investigate the biological role of hsa_circ_0079557 in CRC cells, we constructed si-hsa_circ_0079557 and NC-hsa_circ_0079557 and transfected them into SW480 and SW620 cells. The results of qRT-PCR experiments revealed that the expression of hsa_circ_0079557 was significantly reduced in the si group (Figure 3a). The CCK-8 test was conducted to detect the proliferative ability, while the wound healing and transwell assays were performed to detect the migration ability of CRC cells. In addition, colony formation tests were used to detect the ability of colony formation. We also performed cell cycle experiments and analyzed the results using flow cytometry. The findings revealed that suppression of hsa_circ_0079557 expression significantly inhibited the proliferation and migration of CRC cells and increased the proportion of cells in the G1 phase (Figure 3b-f).

*Hsa_circ_0079557 acts as a "molecular sponge" for miR-502-5p*. Subcellular localization of circRNAs is usually related to their biological functions and molecular mechanisms (22). Studies have reported that circRNAs in the cytoplasm often act as "molecular sponges" for miRNAs (23). We used different databases, including Circinteractome and Circbank, to investigate the regulatory mechanism of has_circ_0079557 in CRC cells and predict potential miRNAs bound by hsa_circ_0079557 (Table S1). We also identified two miRNAs (hsa-miR-502-5p and hsa-miR-330-3p) from the overlapping

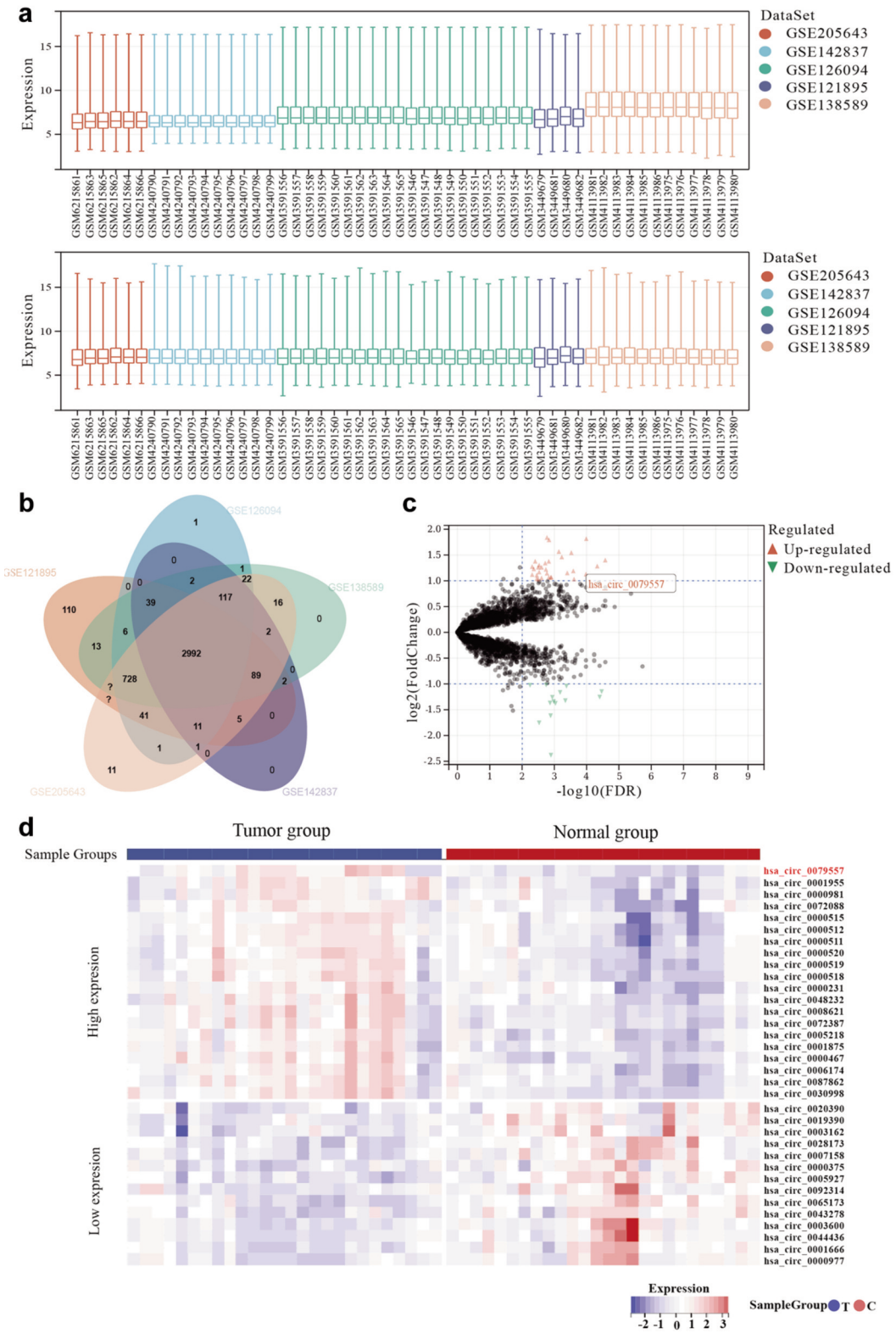


Figure 1. *Bioinformatic analysis shows that hsa_circ_0079557 is relatively highly expressed in colorectal cancer. (a) Batch effect was removed before merging multiple datasets. (b) The Venn diagram shows a new dataset which is composed of GSE205643, GSE142837, GSE126094, GSE121895 and GSE138589. (c) Volcanic map of the new combined dataset is shown. hsa_circ_0079557 is highly expressed in the new dataset. (d) The heatmap demonstrates the distribution of differential expression of genes between samples. Z-score is the normalization used.*

Table III. *limma analysis of the new combined data*.

| Tag | logFC | AveExpr | T | *p*-Value | adj. *p*-Value | B |
|---|---|---|---|---|---|---|
| hsa_circ_0000467 | 1.403365 | 7.666394 | 6.280034 | $6.02\times10^{-8}$ | $2.65\times10^{-5}$ | 8.136678 |
| hsa_circ_0065173 | –1.14873 | 8.306943 | –6.12089 | $1.09\times10^{-7}$ | $3.42\times10^{-5}$ | 7.57919 |
| hsa_circ_0005927 | –1.25591 | 10.67944 | –6.05728 | $1.38\times10^{-7}$ | $3.94\times10^{-5}$ | 7.356918 |
| hsa_circ_0030998 | 1.286773 | 8.734527 | 5.926202 | $2.23\times10^{-7}$ | $4.69\times10^{-5}$ | 6.899995 |
| hsa_circ_0000512 | 1.81767 | 14.38839 | 5.634318 | $6.52\times10^{-7}$ | 0.000103 | 5.889245 |
| hsa_circ_0079557 | 1.130612 | 6.899435 | 5.586434 | $7.76\times10^{-7}$ | 0.000105 | 5.724465 |
| hsa_circ_0008621 | 1.034022 | 7.142169 | 5.156898 | $3.66\times10^{-6}$ | 0.000245 | 4.262828 |
| hsa_circ_0001955 | 1.192849 | 11.94223 | 5.136222 | $3.94\times10^{-6}$ | 0.000259 | 4.193324 |
| hsa_circ_0000519 | 1.546928 | 12.14643 | 5.074508 | $4.91\times10^{-6}$ | 0.000298 | 3.986401 |
| hsa_circ_0006174 | 1.894035 | 10.08315 | 4.975729 | $6.97\times10^{-6}$ | 0.000381 | 3.656922 |
| hsa_circ_0072387 | 1.154877 | 7.731532 | 4.929835 | $8.20\times10^{-6}$ | 0.000397 | 3.504594 |
| hsa_circ_0019390 | –1.04363 | 7.657908 | –4.89733 | $9.19\times10^{-6}$ | 0.00042 | 3.396993 |
| hsa_circ_0028173 | –1.32553 | 10.63803 | –4.86259 | $1.04\times10^{-5}$ | 0.000455 | 3.282322 |
| hsa_circ_0087862 | 1.463068 | 9.53561 | 4.731687 | $1.64\times10^{-5}$ | 0.000588 | 2.852853 |
| hsa_circ_0007158 | –1.1651 | 10.19691 | –4.6462 | $2.21\times10^{-5}$ | 0.000663 | 2.574861 |
| hsa_circ_0000511 | 1.568322 | 14.4759 | 4.591545 | $2.67\times10^{-5}$ | 0.000723 | 2.398198 |
| hsa_circ_0003600 | –1.37744 | 9.501371 | –4.50307 | $3.61\times10^{-5}$ | 0.000925 | 2.114071 |
| hsa_circ_0000375 | –1.34169 | 8.187133 | –4.4467 | $4.38\times10^{-5}$ | 0.001045 | 1.934319 |
| hsa_circ_0003162 | –1.25959 | 8.680728 | –4.40973 | $4.96\times10^{-5}$ | 0.001155 | 1.81695 |
| hsa_circ_0005218 | 1.069081 | 8.07947 | 4.371973 | $5.64\times10^{-5}$ | 0.001237 | 1.697552 |
| hsa_circ_0043278 | –2.38276 | 11.55349 | –4.36032 | $5.87\times10^{-5}$ | 0.001275 | 1.660784 |
| hsa_circ_0048232 | 1.067762 | 8.411905 | 4.346415 | $6.15\times10^{-5}$ | 0.001302 | 1.616995 |
| hsa_circ_0001666 | –1.61792 | 9.93576 | –4.33751 | $6.34\times10^{-5}$ | 0.001302 | 1.588964 |
| hsa_circ_0020390 | –1.37003 | 8.980916 | –4.31662 | $6.80\times10^{-5}$ | 0.001356 | 1.523346 |
| hsa_circ_0000518 | 1.795737 | 11.22429 | 4.282205 | $7.63\times10^{-5}$ | 0.001457 | 1.415578 |
| hsa_circ_0000981 | 1.066732 | 12.55682 | 4.265504 | $8.07\times10^{-5}$ | 0.001484 | 1.36342 |
| hsa_circ_0000520 | 1.378763 | 11.53561 | 4.263333 | $8.13\times10^{-5}$ | 0.001484 | 1.356648 |
| hsa_circ_0072088 | 1.840182 | 12.36045 | 4.206483 | $9.83\times10^{-5}$ | 0.001689 | 1.17988 |
| hsa_circ_0000231 | 1.14759 | 9.395862 | 4.203002 | $9.94\times10^{-5}$ | 0.001693 | 1.169093 |
| hsa_circ_0044436 | –1.02045 | 7.188778 | –4.18126 | 0.000107 | 0.001791 | 1.101813 |
| hsa_circ_0001875 | 1.222292 | 8.76552 | 4.159731 | 0.000115 | 0.001826 | 1.035381 |
| hsa_circ_0000515 | 1.343651 | 13.80191 | 4.129225 | 0.000127 | 0.001917 | 0.941524 |
| hsa_circ_0011385 | 1.055444 | 9.727464 | 4.008306 | 0.000189 | 0.002486 | 0.572966 |
| hsa_circ_0005615 | 1.263324 | 9.323463 | 4.001282 | 0.000193 | 0.002486 | 0.551731 |
| hsa_circ_0003323 | 1.171487 | 9.200086 | 3.921309 | 0.00025 | 0.002953 | 0.311357 |
| hsa_circ_0000514 | 1.30573 | 15.33143 | 3.917069 | 0.000254 | 0.002953 | 0.298687 |
| hsa_circ_0000977 | –1.75634 | 8.037463 | –3.91706 | 0.000254 | 0.002953 | 0.298658 |
| hsa_circ_0005273 | 1.263793 | 9.378593 | 3.888883 | 0.000278 | 0.003144 | 0.214641 |
| hsa_circ_0039929 | 1.031097 | 8.045408 | 3.886631 | 0.00028 | 0.003148 | 0.20794 |
| hsa_circ_0040823 | 1.042813 | 8.951581 | 3.840424 | 0.000324 | 0.003489 | 0.070923 |
| hsa_circ_0075048 | 1.110722 | 7.982795 | 3.838806 | 0.000326 | 0.003495 | 0.066141 |
| hsa_circ_0000517 | 1.379848 | 11.5162 | 3.781889 | 0.000391 | 0.003911 | –0.10134 |
| hsa_circ_0001136 | 1.231551 | 9.320955 | 3.721871 | 0.000473 | 0.004327 | –0.27641 |
| hsa_circ_0000711 | 1.277391 | 9.280525 | 3.659702 | 0.000574 | 0.004859 | –0.45604 |
| hsa_circ_0001727 | 1.121329 | 9.482976 | 3.652314 | 0.000588 | 0.004859 | –0.47727 |
| hsa_circ_0092314 | –1.02621 | 9.095527 | –3.57631 | 0.000744 | 0.005647 | –0.69419 |

results of the two databases (Figure 4a). Subsequent analysis using the TargetScan database and Kyoto KEGG enrichment analysis (Table S2) revealed that miR-502-5p may play a role in CRC and regulate multiple proteins (Figure 4b and c). We measured miR-502-5p expression after the knockdown of hsa_circ_0079557. The results showed that the expression of miR-502-5p in the si-hsa_circ_0079557 group was higher than that in the NC group (Figure 4d). We also observed the subcellular localization of hsa_circ_0079557 and miR-502-5p in CRC cells using the FISH assay. The findings revealed that hsa_circ_0079557 and miR-502-5p primarily exist in the cytoplasm of CRC cells (Figure 4e). Previous studies have also reported miR-502-5p to be involved in breast cancer (24), ovarian cancer (25), bladder cancer (26), and CRC (27).

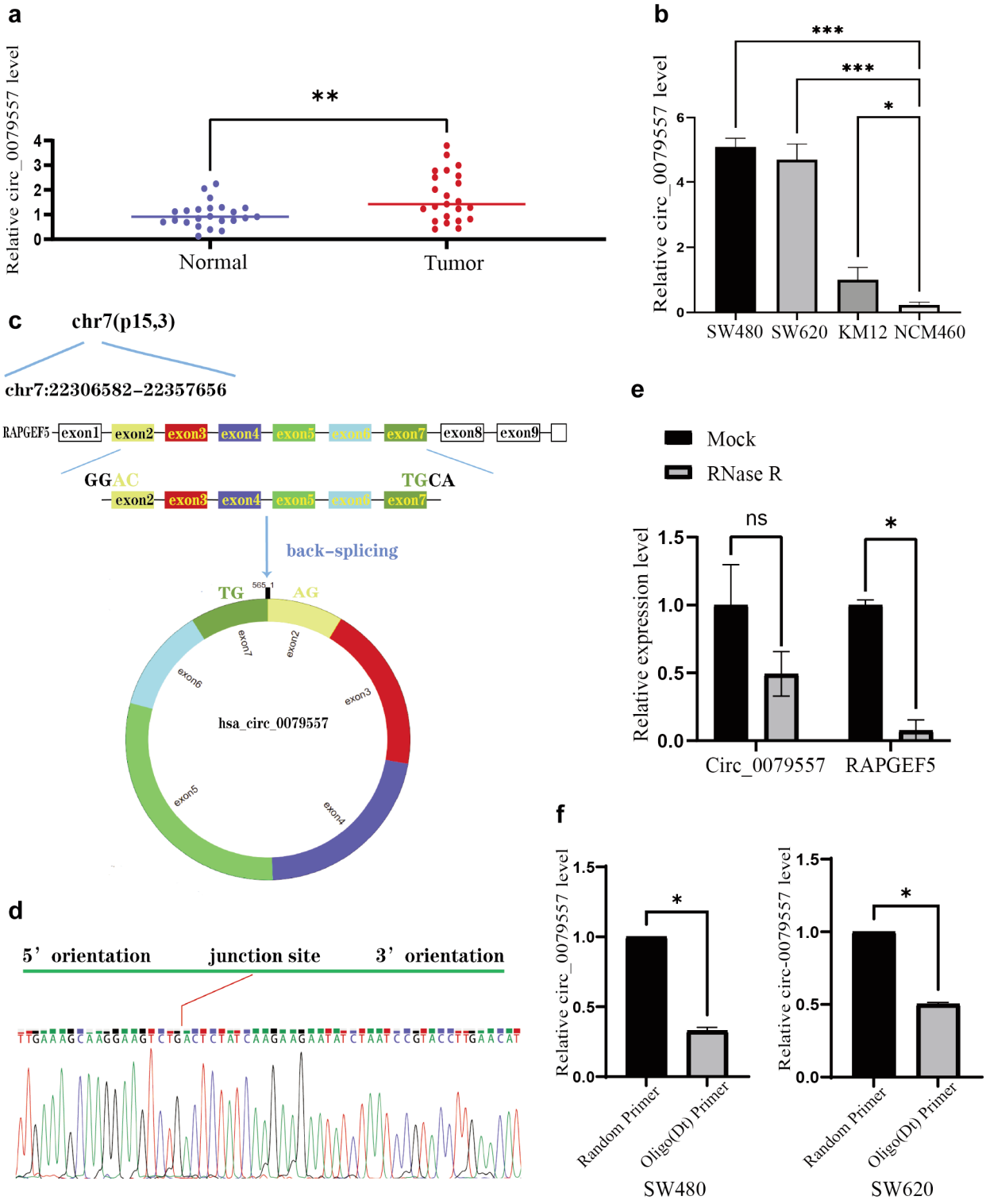


Figure 2. *The expression, stability, and cyclic character of hsa_circ_0079557 in CRC. (a) qRT-PCR analysis of hsa_circ_0079557 expression in CRC tissues and adjacent normal tissues. (b) qRT-PCR analysis of hsa_circ_0079557 expression in CRC cells and normal mucosa cells. (c) Schematic diagram demonstrates formation of hsa_circ_0079557 by circularization of exons 2, 3, 4, 5, 6 and 7 from RAPGEF5 on Chr7 (blue arrow). (d) Sanger sequencing of PCR products of hsa_circ_0079557. The red line indicates the hsa_circ_0079557 splice site. (e) qRT-PCR analysis of the RNA level of hsa_circ_0079557 in RNase R-treated CRC cells. (f) RNA of SW480 and SW620 cells was used for reverse transcription to cDNA with Oligo(dT) primers and mixed primers, respectively. *p<0.05, **p<0.01, ***p<0.001, using t-test and ANOVA followed by Bonferroni correction.*

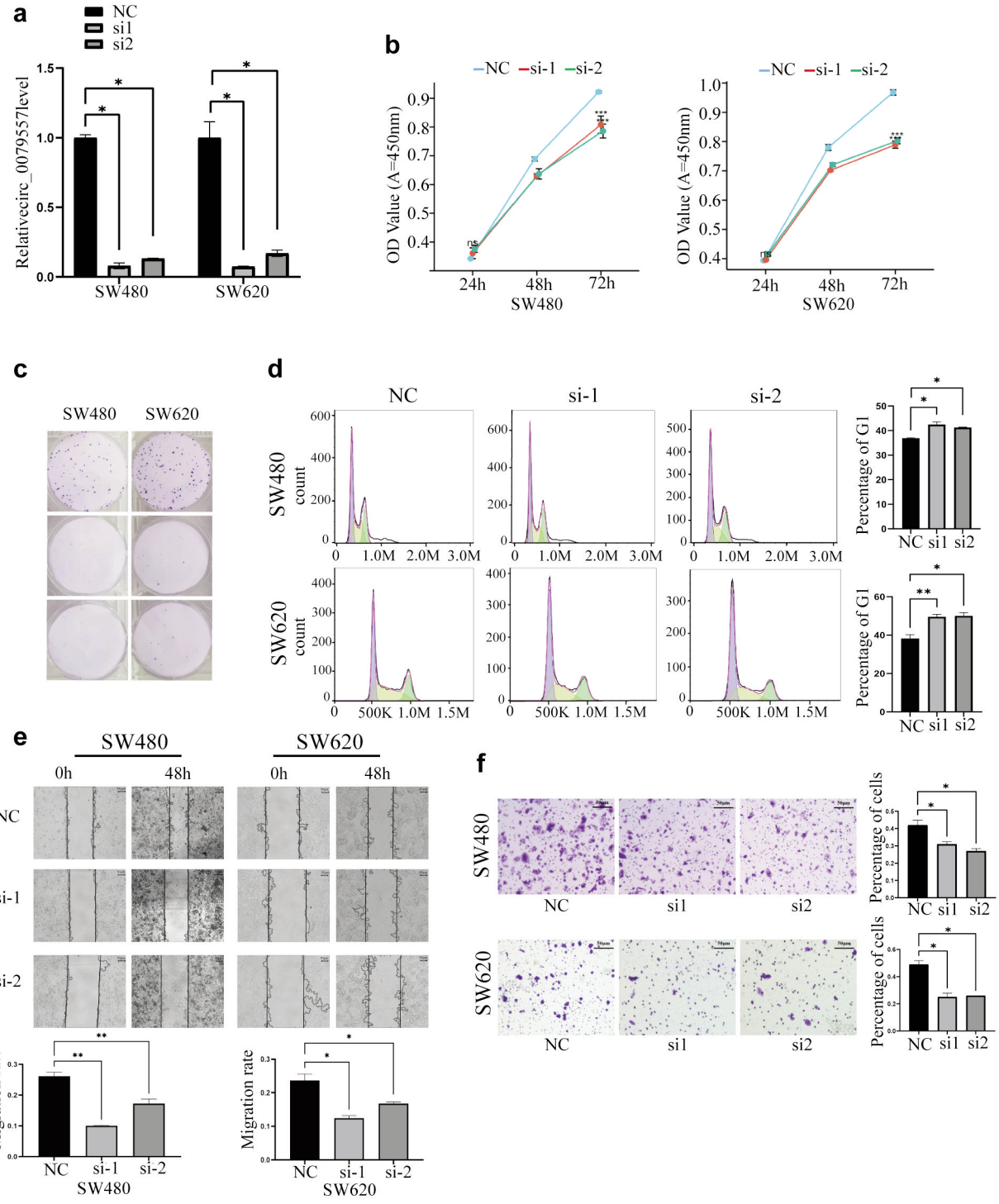


Figure 3. *hsa_circ_0079557 affects the proliferation, migration, colony-forming ability and cell cycle of CRC cells in vitro. (a) Relative expression of hsa_circ_0079557 in SW480 and SW620 cells transfected with si-hsa_circ_0079557 and NC-hsa_circ_0079557. (b) CCK-8 analysis of cell proliferative ability in SW480 and SW620 cells transfected with si-hsa_circ_0079557 or NC-hsa_circ_0079557. (c) Colony assay cells SW480 and SW620 were transfected with si-hsa_circ_0079557 or NC-hsa_circ_0079557. (d) Cell cycle assays in transfected SW480 and SW620 cells. Statistical analysis of the percentage of cells in the G1 phase is shown. (e) Scratch healing assay on transfected SW480 and SW620 cells. A representative image is shown. Statistical analysis of cell migration is shown (scale bar=50 μm). (f) Transwell migration assay in transfected SW480 and SW620 cells. A representative image is shown (scalebar=50 μm). Statistical analysis of cells passing through the transwell filter is shown. *p<0.05, **p<0.01, using ANOVA followed by Bonferroni correction.*

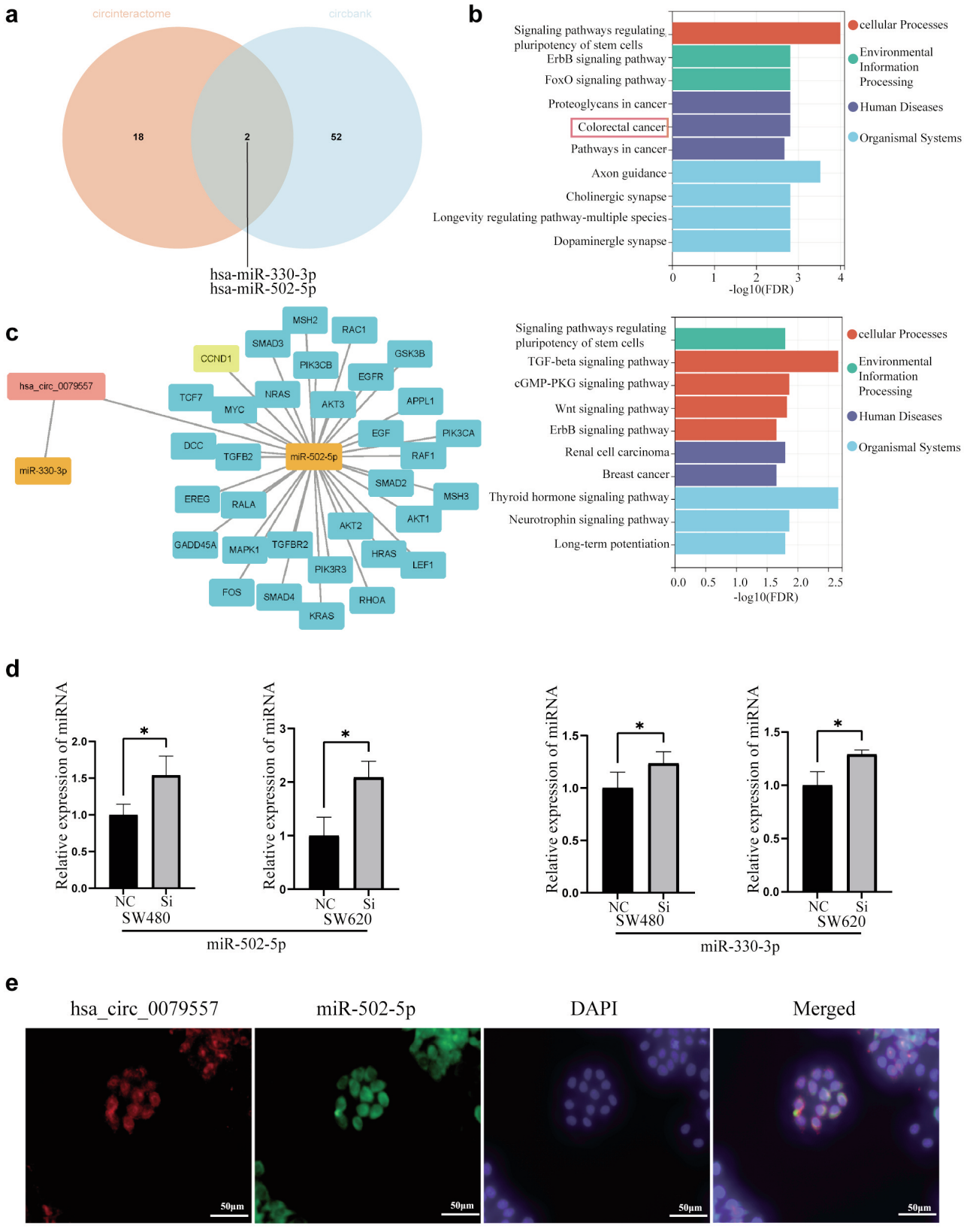


Figure 4. *Continued*

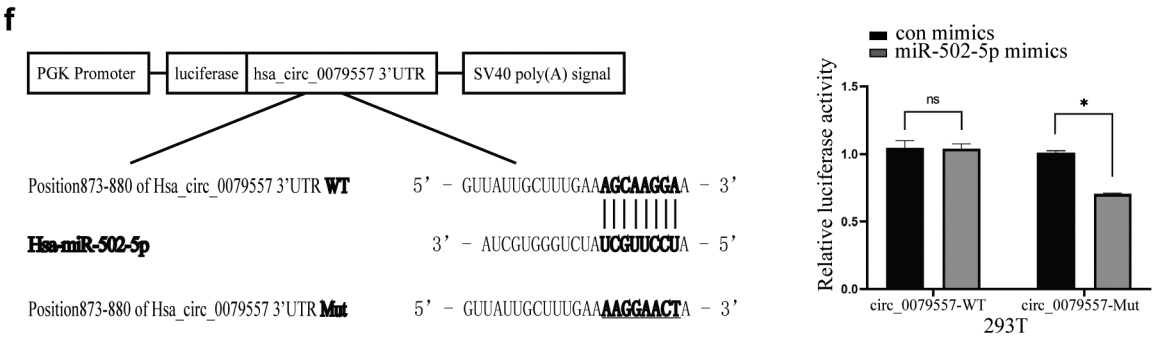


Figure 4. *hsa_circ_0079557 can bind with miR-502-5p. (a) Results of the two databases were intersected to find downstream miRNAs. (b) KEGG analysis of miR-502-5p and miR-330-3p. (c) Prediction of downstream genes binding to miR-502-5p through the TargetScan web-based tool. (d) The expression of miR-502-5p and miR-330-3p after knockdown of hsa_circ_0079557. (e) FISH experiments verified the site of hsa_circ_0079557 and miR-502-5p in CRC cells (scale bar=50 μm). (f) Dual luciferase reporter assays to validate the binding of hsa_circ_0079557 to miR-502-5p. Statistical analysis of relative firefly luciferase activity of wild group and mutant group is shown. Relative luciferase activity is the ratio of firefly luciferase to renilla luciferase. *p<0.05 using t-test.*

According to previous studies, considering the bioinformatics and experimental results, we selected miR-502-5p as the target miRNA of hsa_circ_0079557 for further experiments. We performed a double luciferase assay to determine whether miR-502-5p can directly target hsa_circ_0079557. The results showed that, compared to NC-miR-502-5p, miR-502-5p mimics significantly suppressed the activity of the wild-type luciferase reporter of hsa_circ_0079557. In contrast, the activity of the mutant-type luciferase reporter was not affected by miR-502-5p mimics (Figure 4f). These results indicate that miR-502-5p is the direct target of hsa_circ_0079557 in CRC cells.

*MiR-502-5p promotes the proliferation of CRC cells by targeting CCND1*. After confirming the interaction between hsa_circ_0079557 and miR-502-5p, we investigated the biological role of miR-502-5p in CRC. The results of the bioinformatic analysis suggested that CCND1 is a potential target of miR-502-5p, which has been validated in previous studies (28). To confirm whether miR-502-5p could regulate CCND1 expression in CRC cells, we transfected miR-502-5p mimics or inhibitors into SW480 and SW620 cells and measured CCND1 protein levels using Western blot. The results showed that miR-502-5p mimics decreased CCND1 protein levels in both SW480 and SW620 cells, whereas miR-502-5p inhibitors increased it (Figure 5a).

*Hsa_circ_0079557 could influence the level of CCND1 in CRC cells*. To further determine the regulation of CCND1 expression by hsa_circ_0079557 in CRC cells, we transfected si1-hsa_circ_0079557 and si2-hsa_circ_0079557 into SW480 or SW620 cells, extracted the cell proteins, and performed Western blot experiments. The results showed that the low expression of hsa_circ_0079557 significantly decreased the CCND1 protein levels compared to the NC-hsa_circ_0079557 group (Figure 5b).

*Hsa_circ_0079557 exerts its effect on tumor proliferation via miR-502-5p*. We performed rescue experiments to determine whether hsa_circ_0079557 functions as a tumor-promoting gene through miR-502-5p. We co-transfected si-hsa_circ_0079557 and miR-502-5p inhibitor into CRC cells to determine whether the effect of si-hsa_circ_0079557 could be blocked by the miR-502-5p inhibitor. The results showed that the miR-502-5p inhibitor could partially enhance the proliferation of CRC cells transfected with si-hsa_circ_0079557 (Figure 5c). We also performed Western blot to examine the expression of CCND1 in CRC cells co-transfected with miR-502-5p and si-hsa_circ_0079557. The findings revealed that the down-regulation of CCND1 by si-hsa_circ_0079557 tended to be reduced by the inhibitor of miR-502-5p (Figure 5d).

*Hsa_circ_0079557 impairs tumor growth in vivo*. To further investigate the effect of hsa_circ_0079557 on CRC progression *in vivo*, we performed animal experiments. We injected SW480 cells subcutaneously into nude mice to observe the size of the tumor. The results showed that the tumor volumes were smaller in the sh-hsa_circ_0079557 group than in the NC group (Figure 6a-c). Additionally, the protein expression of CCND1 was detected by IHC (Figure 6d).

*CCND1 is highly expressed in various carcinomas*. According to the UCSC dataset, CCND1 expression is up-regulated in multiple cancers, suggesting that CCND1 is widely involved in the regulation of multiple cancers. This includes breast, colorectal and gastric cancer (Figure 6e).

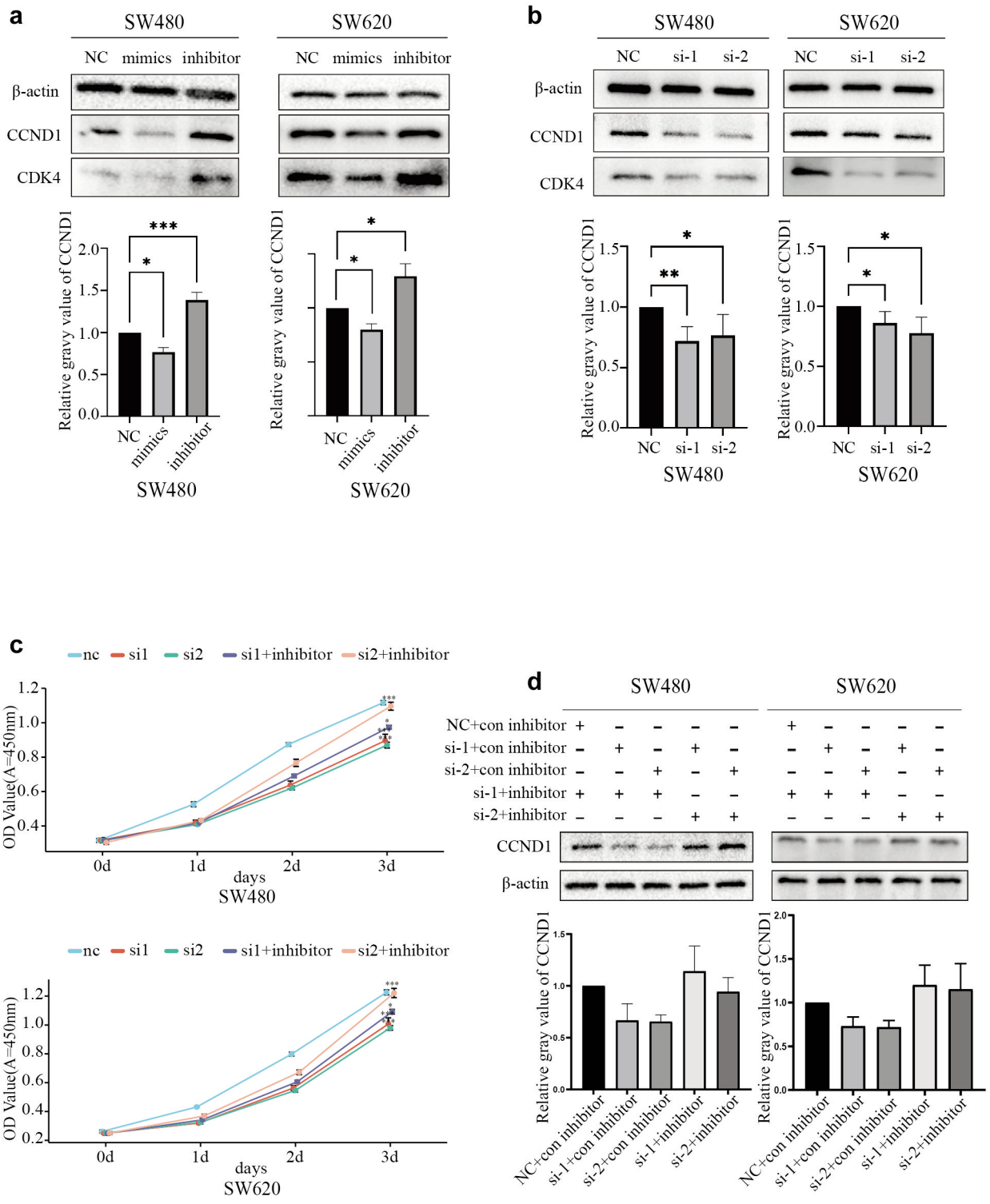


Figure 5. *miR-502-5p can rescue the negative effect of si-hsa_circ_0079557 on cell proliferation and CCND1 expression. (a) Western blot experiments of CCND1 expression levels in CRC cells transfected with miR-502-5p mimics, inhibitor or NC. Statistical analysis of the expression of CCND1 in groups is shown. (b) Western blot experiments of the protein expression levels of CCND1 in CRC cells transfected with si-hsa_circ_0079557 or NC-hsa_circ_0079557. Statistical analysis of the expression of CCND1 in groups is shown. (c) CCK-8 analysis of the cell proliferation ability in co-transfected SW480 and SW620 cells. (d) Western blot experiments of the protein expression level of CCND1 in SW480 and SW620 cells with different co-transfection. *p<0.05, **p<0.01, ***p<0.001 using ANOVA followed by Bonferroni correction.*

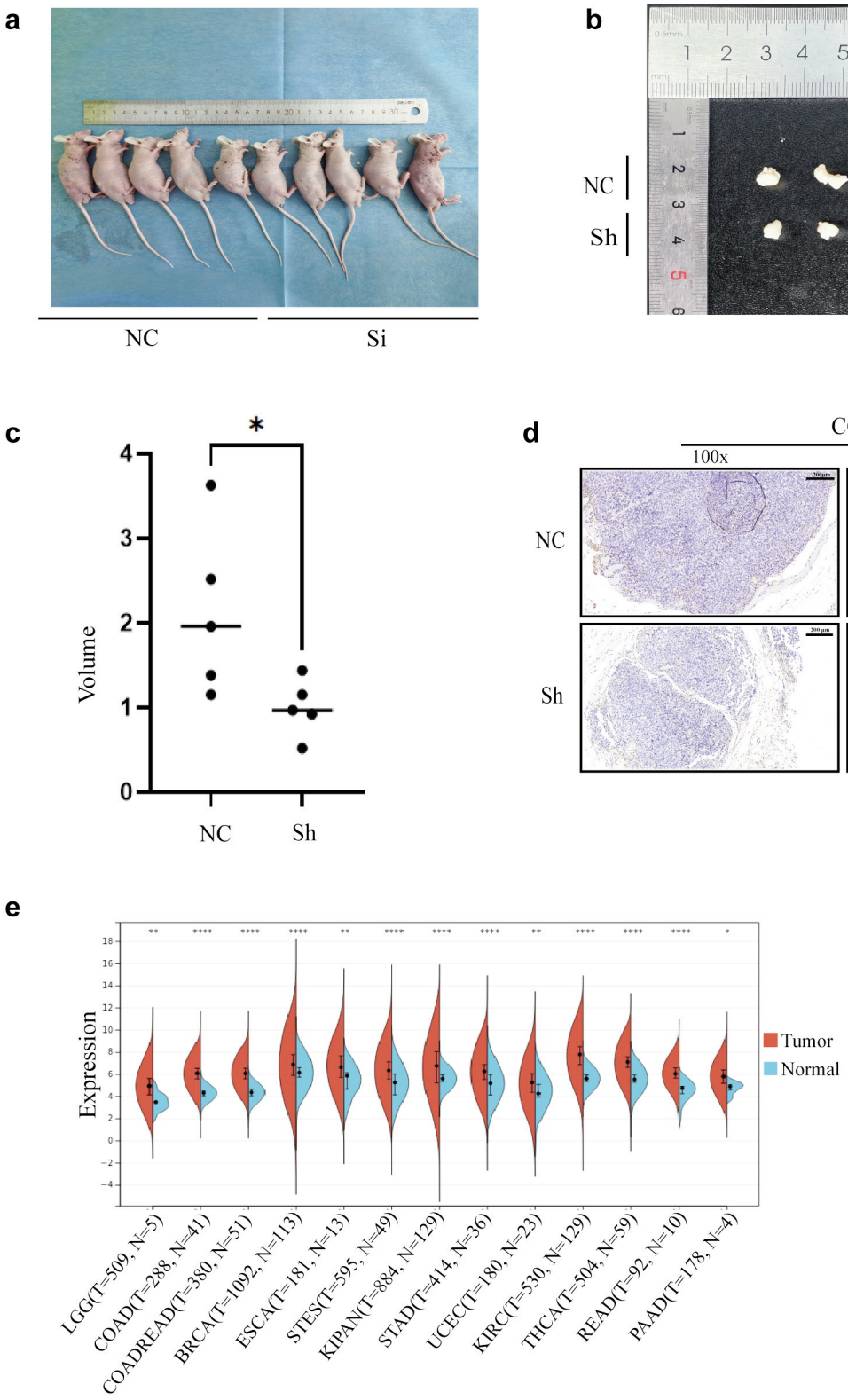


Figure 6. *hsa_circ_0079557 can affect tumor proliferation in vivo. (a) Tumor-bearing mice were photographed. (b) Sectioned tumors are shown. (c) Tumor volumes in groups were statistically analyzed. (d) Images of IHC are shown (scale bars correspond to 50 and 200 μm, respectively). (e) CCND1 expression in 13 cancers. *p<0.05, **p<0.01, ****p<0.0001 using t-test.*

## Discussion

The small sample size of our study may limit the reliability of experimental results. To address this, we conducted a joint analysis by eliminating the difference between datasets. In this study, we analyzed the GEO database and combined five datasets into a new one (Table S3). It was further categorized into the tumor group and the normal group. Our analysis identified some circRNAs that were up-regulated in the tumor group. We verified these highly expressed circRNAs and confirmed that hsa_circ_0079557 was highly expressed in CRC tissues and cells.

Most annotated circRNAs are generated by back-splicing of pre-mRNA (29). Our analysis of the NCBI database showed that hsa_circ_0079557 is generated from the back-splicing of rap guanine nucleotide exchange factor 5 (PAPGEF5) exons 2,3,4,5,6 and 7. CircRNA is a single-stranded RNA with head-to-tail splicing (30); according to this characteristic, the PCR products of circRNAs must be verified. We performed Sanger sequencing to confirm that the qRT-PCR products were specific amplicons of hsa_circ_0079557. The results also confirmed that the products contained the back-splicing junction of hsa_circ_0079557. Moreover, most circRNAs remain stable (31), possibly due to their resistance to degradation by the linear RNA decay machinery. Furthermore, hsa_circ_0079557 was more stable than linear RNA and was relatively difficult to be degraded by RNase R. Exonic circRNAs are usually located in the cytoplasm (32), and our FISH experiment confirmed that hsa_circ_0079557 is mainly present there. Additionally, we verified that the down-regulation of hsa_circ_0079557 inhibited the migration and proliferation of CRC cells, indicating that hsa_circ_0079557 has functional significance beyond its high expression in tumors.

Many circRNAs play essential biological roles as microRNA or protein inhibitors (sponges) either by regulating protein function or translation (30). We found that hsa_circ_0079557 could bind to miR-502-5p and affect its expression. It has previously been reported that CCND1 is a direct target of miR-502-5p (26). CCND1 plays a critical role in the cell cycle and can affect cell cycle progression (33). The results of the cell cycle experiment were consistent with the function of CCND1. Thus, we repeated the experiment to demonstrate the effect of miR-502-5p on CCND1 in CRC cells. The results showed that miR-502-5p could inhibit CCND1 expression, so we speculated that hsa_circ_0079557 could also regulate CCND1 expression probably by regulating miR-502-5p; this was confirmed by Western blot and rescue experiments. Based on these findings, we propose that hsa_circ_0079557 may promote CCND1 expression by sponging miR-502-5p, thereby promoting the proliferation of CRC *in vitro*.

Furthermore, we observed that tumor volumes of the sh-hsa_circ_0079557 group were significantly smaller than those of the NC group by performing experiments with nude mice. The results further confirmed that hsa_circ_0079557 plays an essential role in CRC cell proliferation *in vivo*. Subsequently, subcutaneous tumors were subjected to IHC, and the results showed that CCND1 was highly expressed in the NC group compared with its expression in the sh-hsa_circ_0079557 group. Therefore, we regarded that the novel pathway of hsa_circ_0079557/miR-502-5p/CCND1 is also functional *in vivo*.

In summary, in this study, we investigated the expression of the circRNAs in CRC *via* GEO databases. Our results showed that some circRNAs could be up-regulated in CRC tissues compared with normal tissues. Experimentally, we confirmed that hsa_circ_0079557 is highly expressed in CRC and plays a role in CRC proliferation and migration. Furthermore, through bioinformatic analysis and experiments, miR-502-5p was found to be a target of hsa_circ_0079557 and affected its function in CRC. Moreover, we demonstrated that the low expression of hsa_circ_0079557 could reduce the expression of CCND1 through miR-502-5p *in vitro* and *in vivo*.

## Conclusion

Our findings revealed that hsa_circ_0079557 promotes the proliferation of CRC cells by acting as a miR-502-5p sponge and influencing the expression of CCND1. We propose a novel pathway of hsa_circ_0079557/miR-502-5p/CCND1 in CRC which may provide a new target for diagnosing and treating CRC. In the future, studies on drugs targeting this pathway for treating CRC could also be of interest.

## Conflicts of Interest

The Authors declare that they have no conflicts of interest.

## Authors' Contributions

YJL and YC conceived and designed the study; YC and HX performed the experiments; YC performed the data analyses and wrote the manuscripts. YJL, HRL, WPQ, CZD, LQN and CHD reviewed and edited the manuscript. All Authors read and approved the manuscript.

## Acknowledgements

We would like to thank "sangerbox" for providing a comprehensive and interactive clinical bioinformatics analysis platform (https://doi.org/10.1002/imt2.36). This study was funded by Science and Technology Planning Project of Guangdong Province (Grant number 2019B030316011).

## Supplementary Material

Supplementary documents can be obtained from the following links: Table S1: https://share.weiyun.com/2Px3BHgq; Table S2: https://share.weiyun.com/iE2zJhkl; Table S3: https://share.weiyun.com/AM4xRgXT

## References


1 Sung H, Ferlay J, Siegel RL, Laversanne M, Soerjomataram I, Jemal A, Bray F: Global cancer statistics 2020: GLOBOCAN estimates of incidence and mortality worldwide for 36 cancers in 185 countries. CA Cancer J Clin 71(3): 209-249, 2021. DOI: 10.3322/caac.21660

2 Arnold M, Sierra MS, Laversanne M, Soerjomataram I, Jemal A, Bray F: Global patterns and trends in colorectal cancer incidence and mortality. Gut 66(4): 683-691, 2017. DOI: 10.1136/gutjnl-2015-310912

3 Wang GR, Wang ZW, Jin ZY: Application and progress of texture analysis in the therapeutic effect prediction and prognosis of neoadjuvant chemoradiotherapy for colorectal cancer. Chin Med Sci J 34(1): 45-50, 2019. DOI: 10.24920/003572

4 Bertocchi A, Carloni S, Ravenda PS, Bertalot G, Spadoni I, Lo Cascio A, Gandini S, Lizier M, Braga D, Asnicar F, Segata N, Klaver C, Brescia P, Rossi E, Anselmo A, Guglietta S, Maroli A, Spaggiari P, Tarazona N, Cervantes A, Marsoni S, Lazzari L, Jodice MG, Luise C, Erreni M, Pece S, Di Fiore PP, Viale G, Spinelli A, Pozzi C, Penna G, Rescigno M: Gut vascular barrier impairment leads to intestinal bacteria dissemination and colorectal cancer metastasis to liver. Cancer Cell 39(5): 708-724.e11, 2021. DOI: 10.1016/j.ccell.2021.03.004

5 Franke AJ, Skelton WP, Starr JS, Parekh H, Lee JJ, Overman MJ, Allegra C, George TJ: Immunotherapy for colorectal cancer: a review of current and novel therapeutic approaches. J Natl Cancer Inst 111(11): 1131-1141, 2019. DOI: 10.1093/jnci/djz093

6 Lei X, He Q, Li Z, Zou Q, Xu P, Yu H, Ding Y, Zhu W: Cancer stem cells in colorectal cancer and the association with chemotherapy resistance. Med Oncol 38(4): 43, 2021. DOI: 10.1007/s12032-021-01488-9

7 Yan H, Bu P: Non-coding RNA in cancer. Essays Biochem 65(4): 625-639, 2021. DOI: 10.1042/EBC20200032

8 Yu T, Wang Y, Fan Y, Fang N, Wang T, Xu T, Shu Y: CircRNAs in cancer metabolism: a review. J Hematol Oncol 12(1): 90, 2019. DOI: 10.1186/s13045-019-0776-8

9 Xu X, Zhang J, Tian Y, Gao Y, Dong X, Chen W, Yuan X, Yin W, Xu J, Chen K, He C, Wei L: CircRNA inhibits DNA damage repair by interacting with host gene. Mol Cancer 19(1): 128, 2020. DOI: 10.1186/s12943-020-01246-x

10 Liu Z, Gu S, Wu K, Li L, Dong C, Wang W, Zhou Y: CircRNA-DOPEY2 enhances the chemosensitivity of esophageal cancer cells by inhibiting CPEB4-mediated Mcl-1 translation. J Exp Clin Cancer Res 40(1): 361, 2021. DOI: 10.1186/s13046-021-02149-5

11 Pan Z, Zhao R, Li B, Qi Y, Qiu W, Guo Q, Zhang S, Zhao S, Xu H, Li M, Gao Z, Fan Y, Xu J, Wang H, Wang S, Qiu J, Wang Q, Guo X, Deng L, Zhang P, Xue H, Li G: EWSR1-induced circNEIL3 promotes glioma progression and exosome-mediated macrophage immunosuppressive polarization *via* stabilizing IGF2BP3. Mol Cancer 21(1): 16, 2022. DOI: 10.1186/s12943-021-01485-6

12 Zhang H, Jiang L, Sun D, Hou J, Ji Z: CircRNA: a novel type of biomarker for cancer. Breast Cancer 25(1): 1-7, 2018. DOI: 10.1007/s12282-017-0793-9

13 Yang H, Li X, Meng Q, Sun H, Wu S, Hu W, Liu G, Li X, Yang Y, Chen R: CircPTK2 (hsa_circ_0005273) as a novel therapeutic target for metastatic colorectal cancer. Mol Cancer 19(1): 13, 2020. DOI: 10.1186/s12943-020-1139-3

14 Xu H, Liu Y, Cheng P, Wang C, Liu Y, Zhou W, Xu Y, Ji G: CircRNA_0000392 promotes colorectal cancer progression through the miR-193a-5p/PIK3R3/AKT axis. J Exp Clin Cancer Res 39(1): 283, 2020. DOI: 10.1186/s13046-020-01799-1

15 He J, Chu Z, Lai W, Lan Q, Zeng Y, Lu D, Jin S, Xu H, Su P, Yin D, Chu Z, Liu L: Circular RNA circHERC4 as a novel oncogenic driver to promote tumor metastasis *via* the miR-556-5p/CTBP2/E-cadherin axis in colorectal cancer. J Hematol Oncol 14(1): 194, 2021. DOI: 10.1186/s13045-021-01210-2

16 Thomson DW, Dinger ME: Endogenous microRNA sponges: evidence and controversy. Nat Rev Genet 17(5): 272-283, 2016. DOI: 10.1038/nrg.2016.20

17 Xu H, Liu Y, Cheng P, Wang C, Liu Y, Zhou W, Xu Y, Ji G: CircRNA_0000392 promotes colorectal cancer progression through the miR-193a-5p/PIK3R3/AKT axis. J Exp Clin Cancer Res 39(1): 283, 2020. DOI: 10.1186/s13046-020-01799-1

18 Zhou C, Liu HS, Wang FW, Hu T, Liang ZX, Lan N, He XW, Zheng XB, Wu XJ, Xie D, Wu XR, Lan P: circCAMSAP1 promotes tumor growth in colorectal cancer *via* the miR-328-5p/E2F1 axis. Mol Ther 28(3): 914-928, 2020. DOI: 10.1016/j.ymthe.2019.12.008

19 Champeris Tsaniras S, Delinasios GJ, Petropoulos M, Panagopoulos A, Anagnostopoulos AK, Villiou M, Vlachakis D, Bravou V, Stathopoulos GT, Taraviras S: DNA replication inhibitor geminin and retinoic acid signaling participate in complex interactions associated with pluripotency. Cancer Genomics Proteomics 16(6): 593-601, 2019. DOI: 10.21873/cgp.20162

20 Johnson WE, Li C, Rabinovic A: Adjusting batch effects in microarray expression data using empirical Bayes methods. Biostatistics 8(1): 118-127, 2007. DOI: 10.1093/biostatistics/kxj037

21 Livak KJ, Schmittgen TD: Analysis of relative gene expression data using real-time quantitative PCR and the $2-\Delta\Delta CT$ method. Methods 25(4): 402-408, 2001. DOI: 10.1006/meth.2001.1262

22 Lu Q, Liu T, Feng H, Yang R, Zhao X, Chen W, Jiang B, Qin H, Guo X, Liu M, Li L, Guo H: Circular RNA circSLC8A1 acts as a sponge of miR-130b/miR-494 in suppressing bladder cancer progression *via* regulating PTEN. Mol Cancer 18(1): 111, 2019. DOI: 10.1186/s12943-019-1040-0

23 Kristensen LS, Andersen MS, Stagsted LVW, Ebbesen KK, Hansen TB, Kjems J: The biogenesis, biology and characterization of circular RNAs. Nat Rev Genet 20(11): 675-691, 2019. DOI: 10.1038/s41576-019-0158-7

24 Li J, Gao X, Zhang Z, Lai Y, Lin X, Lin B, Ma M, Liang X, Li X, Lv W, Lin Y, Zhang N: CircCD44 plays oncogenic roles in triple-negative breast cancer by modulating the miR-502-5p/KRAS and IGF2BP2/Myc axes. Mol Cancer 20(1): 138, 2021. DOI: 10.1186/s12943-021-01444-1

25 Zhan L, Yang J, Liu Y, Cheng Y, Liu H: MicroRNA miR-502-5p inhibits ovarian cancer genesis by downregulation of GINS complex subunit 2. Bioengineered 12(1): 3336-3347, 2021. DOI: 10.1080/21655979.2021.1946347

26 Ying Y, Li J, Xie H, Yan H, Jin K, He L, Ma X, Wu J, Xu X, Fang J, Wang X, Zheng X, Liu B, Xie L: CCND1, NOP14 and DNMT3B are involved in miR-502-5p-mediated inhibition of cell migration and proliferation in bladder cancer. Cell Prolif 53(2): e12751, 2020. DOI: 10.1111/cpr.12751

27 Zhai H, Song B, Xu X, Zhu W, Ju J: Inhibition of autophagy and tumor growth in colon cancer by miR-502. Oncogene 32(12): 1570-1579, 2013. DOI: 10.1038/onc.2012.167

28 Abuduhadeer X, Maimaiti Y, Kamali A, Yang P, Zhong K: Hsa_circ_0008092 contributes to cell proliferation and metastasis in hepatocellular carcinoma *via* the miR-502-5p/CCND1 axis. Protein Pept Lett 29(7): 595-604, 2022. DOI: 10.2174/0929866529666220721090209
29 Liu C, Chen L: Circular RNAs: Characterization, cellular roles, and applications. Cell 185(12): 2016-2034, 2022. DOI: 10.1016/j.cell.2022.04.021
30 Chen L, Shan G: CircRNA in cancer: Fundamental mechanism and clinical potential. Cancer Lett 505: 49-57, 2021. DOI: 10.1016/j.canlet.2021.02.004
31 Zhang Y, Xue W, Li X, Zhang J, Chen S, Zhang J, Yang L, Chen L: The biogenesis of nascent circular RNAs. Cell Rep 15(3): 611-624, 2016. DOI: 10.1016/j.celrep.2016.03.058
32 Hsu M, Coca-prados M: Electron microscopic evidence for the circular form of RNA in the cytoplasm of eukaryotic cells. Nature 280(5720): 339-340, 1979. DOI: 10.1038/280339a0
33 Zhu D, Huang J, Liu N, Li W, Yan L: PSMC2/CCND1 axis promotes development of ovarian cancer through regulating cell growth, apoptosis and migration. Cell Death Dis 12(8): 730, 2021. DOI: 10.1038/s41419-021-03981-5

*Received June 2, 2023*
*Revised July 22, 2023*
*Accepted August 4, 2023*